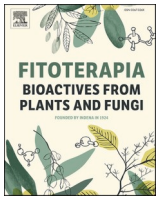
Fitoterapia 176 (2024) 106037



Contents lists available at ScienceDirect

Fitoterapia

journal homepage: www.elsevier.com/locate/fitote



Phytochemicals and enzymes inhibitory potentials of leaves and rootbarks of *Sarcocephallus latifolius* (smith): *In vitro* and *in silico* investigations

Abdulfatai Temitope Ajiboye [a,b,c,*], Olayinka Taiwo Asekun [b], Yusuf Oloruntoyin Ayipo [a,d], Mohd Nizam Mordi [d], Oluwole Babafemi Familoni [b], Zulfiqar Ali [c], Ikhlas A. Khan [c]

[a] Department of Chemistry and Industrial Chemistry, Faculty of Pure and Applied Sciences, PMB 1530, Kwara State University, Malete, Nigeria
[b] Department of Chemistry, Faculty of Science, University of Lagos, Nigeria
[c] National Center for Natural Products Research, School of Pharmacy, University of Mississippi, University, MS 38677, United States
[d] Centre for Drug Research, Universiti Sains Malaysia, USM, 11800, Pulau Pinang, Malaysia

ARTICLE INFO

Keywords:
Diabetes mellitus
Hyperglycemia
α-Amylase and α-glucosidase
Molecular docking, inhibitory assays
Sarcocephalus latifolius

ABSTRACT

In this study, bioactive compounds were isolated and characterized from the leaves and root-barks extracts of *S. latifolius*, with subsequent *in vitro* experimental investigations for antihyperglycemic potentials on α-amylase and α-glucosidase enzymes. Thirteen bioactive compounds were identified, including 10-Hydroxystrictosamide (2) and Quinovic acid-3-O-α-L-rhamnosyl-28-O-β-D-glucopyranosyl ester (8), using chromatographic, nuclear magnetic resonance spectroscopy (NMR), and mass spectrometry (MS) techniques. Experimental assays revealed that compounds 1–4 exhibited potent inhibition of α-amylase and α-glucosidase, with compound 2 demonstrating the most potent α-amylase inhibition (IC_{50} value of 0.52 ± 0.003 μg/mL). Compound 8 showed a lower IC_{50} value (0.098 ± 0.016 μg/mL) against α-glucosidase compared to compound 2 and acarbose. Synergistic effects among the compounds could enhance their inhibitory actions on the enzymes, positioning them as potential anti-hyperglycemia agents. Compound 2 displayed the highest binding affinity (−7.970 kcal/mol) when docked against α-amylase (PDB ID: 2QV4), comparable to acarbose (−8.515 kcal/mol). It also ranked among the top ligands against α-glucosidase (PDB ID 3TOP), although compound 13 and acarbose had higher docking scores. All compounds exhibited ideal ADMET properties, suggesting good bioavailability and low toxicity. In conclusion, the isolated compounds exhibit promising antihyperglycemic potential and favourable safety profiles for further exploration.

1. Introduction

Diabetes mellitus remains a major metabolic disorder with a complex aetiology. It is inclusively characterized by various pathomechanisms including insufficient production of insulin in the pancreas, engendering high blood sugar (hyperglycemia) [1]. It is currently affecting hundreds of millions of the global population, with a forecasted alarming epidemiology by 2030 and 2045 [2]. Its clinical conditions are complicated by efficacious challenges and unpleasant aftereffects associated with the currently available medications. In addition, the complexity surrounding its aetiology implicates several targets including two prominent human pancreatic enzymes, σ-amylase and α-glucosidase. These are enzymes renowned for the hydrolysis of the 1,4-glycosidic linkages in dietary carbohydrates, converting them into monosaccharides that can be internally absorbed in humans. They represent plausible targets for relevant diseases such as obesity and type 2 diabetes (T2D) [3,4]. Inhibitors of the enzyme are amenable to suppressing starch hydrolysis and thereby applied as drug molecules for such diseases, notably, diabetes where they act as oral hypoglycemic medications [5]. A renowned inhibitor in clinical applications for treating type 2 diabetes through these pathways is acarbose [6]. It prevents and delays the development of impaired glucose tolerance (IGT) and hyperglycemia, prediabetic clinical conditions [5]. It also retards the rates of digestion of carbohydrates and downregulates the spiking of postprandial blood sugar levels, a condition associated with the on-set development and progression of some chronic morbidity- and mortality-inclined conditions including ageing and T2D [7]. However, some serious side effects such as abdominal pain, diarrhoea and flatulence have been reported among the

* Corresponding author at: Department of Chemistry and Industrial Chemistry, Faculty of Pure and Applied Sciences, PMB 1530, Kwara State University, Malete, Nigeria.
E-mail address: abdulfatai.ajiboye@kwasu.edu.ng (A.T. Ajiboye).

https://doi.org/10.1016/j.fitote.2024.106037
Received 5 February 2024; Received in revised form 17 May 2024; Accepted 24 May 2024
Available online 25 May 2024
0367-326X/© 2024 Elsevier B.V. All rights are reserved, including those for text and data mining, AI training, and similar technologies.

drawbacks of the drug. As such, patients with pre-existing clinical conditions such as severe gastrointestinal and kidney dysfunctions are usually restricted from taking the drug [8]. Moreover, a meta-analysis has shown that its efficacy and tolerance in T2D patients debatably appear ethnicity-dependent [5]. These significantly affect the applicability of acarbose and warrant further search for better alternatives with improved efficacy, tolerance, and milder aftereffects. Progressively, a natural flavonoid, baicalein has been reported as a promising adjuvant that can ameliorate the intestinal side effects of acarbose [9], stemming the exploring of other dietary natural bioactive agents as future inhibitors of α-amylase and α-glucosidase inhibitors for T2D management.

The *Sarcocephallus* genus is native to Africa and Asia [10]. *Sarcocephallus* (*Nauclea*) *latifolius* is one of the most important genera of *Rubiaceae,* known for various medicinal activities. Many studies have reported different biological activities of extracts from various parts of this plant [11–15]. Monoterpene indole alkaloid is the major phytochemical constituent of *S. latifolius* [16]. Other phytochemicals such as saponins [17–19], phenols [12,18,20–22] and pentacyclic triterpenoids [23] have been reported from *S. latifolius* extracts. Relevantly, their presence has facilitated inhibitory potentials of the extracts on various disease-related enzymes such as acetylcholinesterase, α-amylase and α-glucosidase thereby supporting the medicinal effects as antioxidant, antidiabetics.

In this study, the isolation, identification and structure elucidation of phenolic acids, flavonoid glycoside, monoterpene indole alkaloids, saponins (mono and bis-desmosides), pentacyclic triterpenoid and steroids from the leaves and root-bark extracts of *S. latifolius* respectively were conducted. Experimentally, the isolated compounds were investigated *in vitro* for enzyme inhibitory actions against α-amylase and α-glucosidase. Furthermore, docking analysis was applied to observe the mode of mechanistic binding interactions between the selected compounds and active site residues of both enzymes. In addition, the selected compounds were predicted for druggability and toxicity, consistently with some relevant studies [24].

2. Experimental section

2.1. General experimental procedures

NMR spectra were obtained on Bruker AU III 400 or 500 MHz NMR spectrometers using DMSO-d_6, CD_3OD, or $CDCl_3$ solvents. An Agilent Technologies 6200 series mass spectrometer were used to record mass spectra. TLC was performed on aluminum-backed plates, pre-coated with silica gel F_{254} (200 μm, 60 Å, (Merck). Spots were detected at UV-254 nm. Visualization was attained by spraying with 1% vanillin solution (prepared with 5% H_2SO_4 in ethanol) followed by heating. Methanol, ethanol, acetone, ethylacetate, n-hexane, chloroform, α-amylase, α-glucosidase, 3,5-dinitrosalicylic acid, tetraoxosulphate VI acid (H_2SO_4) para-nitroxyl-α-D-glucopyranoside, starch, vanillin reagent BDH (Poole, England). All other chemicals and solvents used were of analytical grade.

2.2. Plant materials

The leaves and root of *Sarcocephelus latifolius* were collected in April 2017 from Kwara State University environ, Malete, Nigeria (8^0 42′ 35.9215″N, 4^0 27′59.5904″E), because it is grown abundantly in this region. The plant was taxonomically identified and authenticated by Mr. Odewo A. Samuel (Department of Forest Conversation and Protection, Forestry Research Institute of Nigeria (FRIN)), Ibadan Oyo State, Nigeria, where its voucher specimen (FHI 112260) was deposited. A voucher specimen (#20831) was also deposited at the National Centre for Natural Products Research, University of Mississippi, USA [17]. The leaves and root bark parts of *S. latifolius* were prepared for extraction by cleaning, drying for 7 days and pulverized.

2.3. Extraction and isolation

2.3.1. Leaves

The air-dried pulverized leaves of *S. latifolius* (1.6 kg) were extracted in methanol (95%) by percolation method of extraction at room temperature for 72 h. The extract was drained off and the residue was re-extracted (3 × 5 L × 72 h) in the same manner with a fresh batch of methanol. The collected filtrates were pooled and concentrated *in vacuo* at 40 °C to afford 256 g (16.0%) crude extract (dark-green solid). The residue (240 g) was subjected to vacuum liquid chromatography (VLC) loaded with a reverse phase silica (C-18) and eluted successfully with the gradient of methanol-water (0:100 to 100:0) and finally with acetone (100%) to obtain 12 fractions (Fr.1–12). The progress of column was monitored by TLC of the resulting fractions and spots were visualized by employing a UV light (254 and 360 nm) as well as by heating after vanillin-H_2SO_4 reagent spray. The fractions were pooled into three sub-fractions (A-C) based on their TLC profile pattern to give a brown syrup like substance A (97 g), reddish brown gummy like substance B (61 g) and greenish solid C (42 g). Sub-fraction B (26 g) was further fractionated over a Sephadex LH-20 column chromatography (CC) and eluted with methanol (100%) to obtain 24 fractions which were pooled to give 3 sub-fractions (B_1-B_3). B_2 (5.0 g) was loaded onto a silica gel CC and eluted with $CHCl_3$/EtOAc/MeOH/H_2O (4:6:4:1) to yield 4 sub-fractions Bi (500 mg), Bii (724.7 mg), Biii (162.7 mg) and Biv (435.1 mg). Bi (500 mg) was repeatedly subjected to silica gel CC, eluted with $CHCl_3$/EtOAc/MeOH/H_2O (4:6:4:1) and further purified on a Sephadex LH-20 cc with MeOH (100%) to obtain **Compound 1** (32.5 mg) and a mixture of two compounds (105.8 mg). Bii was first chromatographed on a silica gel CC, eluting with $CHCl_3$/EtOAc/MeOH/H_2O (4:6:4:1) and then purified on a Sephadex LH-20 cc, eluted with MeOH (100%) to afford **Compound 2** (42 mg) and an unidentified orange compound (20.0 mg). Fraction B_3 (1.0 g) was loaded on to a silica gel column and eluted with $CHCl_3$/EtOAc/MeOH/H_2O (4:6:4:1) to yield two fractions which were repeatedly purified on Sephadex LH-20 CC eluting with (MeOH 100%) to obtain **Compound 3** (157.6 mg) and **Compound 4** (5.2 mg) respectively.

2.3.2. Rootbarks

The air-dried pulverized root bark of *S. latifolius* (500 g) was extracted in 95% ethanol at ambient temperature for 72 h by maceration. The extract was filtered, and the residue was re-extracted thrice in the same manner with a fresh batch of solvent. The collected filtrates were pooled and concentrated *in vacuo* at 40 °C to afford 20.0 g (4.0%), a brown gummy crude extract which was coded as ERS (Ethanolic root extract of *S. latifolius*).

An aliquot of the ERS (8.0 g) was subjected to column chromatography (CC) over a normal silica gel (230–400 mesh) and eluted with a combination of solvents chloroform/ethyl acetate/methanol/water (8:15:2:0.5). The progress of column was monitored by TLC of the resulting fractions and spots were visualized by employing a UV light (254 and 360 nm) as well as by heating after vanillin-H_2SO_4 reagent spray. Column fractions were combined based on the TLC pattern to afford six fractions (A-F). Fraction B (300.3 mg) was loaded onto a silica gel column (60 cm × 2.5 cm), eluted first with $CHCl_3$ (100%) and $CHCl_3$/MeOH (95:5) to afford **Compounds 5** (25.1) and **6** (18.0) respectively. Fraction C (262.2 mg) was loaded onto a silica gel column (60 cm × 2.5 cm), eluted with chloroform/ethyl acetate/methanol/water (8:15:2:0.5) to afford 10 fractions which were further pooled to afford two sub-fractions (C1 and C2) based on their TLC profile. Fraction C1 (20.2 mg) was further purified over a Sephadex LH-20 column with methanol to give **Compound 7** (6.7 mg). Fraction D (250.4 mg) was chromatographed over a silica gel column (56 cm × 2.5 cm) with chloroform/ethyl acetate/methanol/water (8:15:2:0.5) to give eight fractions which were pooled to three sub-fractions (D1-D3). Fractions D1 (15.5 mg) and D2 (38.2 mg) were further purified by Sephadex LH-20 (20 cm × 0.5 cm) CC with methanol as eluting solvent to afford

Compound 8 (5.6 mg) and **Compound 9** (6.0 mg), respectively. Fraction D3 (120.3 mg) afforded **Compound 10** (64.4 mg) after being chromatographed over a silica gel column (56 cm × 2.5 cm) with chloroform/ethyl acetate/methanol/water (4:6:4:1), followed by purification over Sephadex LH-20 (40 × 2.5 cm) CC with methanol. **Compounds 11** (7.1 mg) and **12** (13.6 mg) were purified from Fr. E (150.4 mg) by repeated CC [silica gel (56 cm × 2.5), chloroform/ethyl acetate/methanol/water (4:6:4:1)] and [Sephadex LH-20 (20 cm × 0.5 cm), methanol]. Compound **13** (15.9 mg) was purified from fraction F by CC over a Sephadex LH-20 (56 × 2.5 cm) with methanol.

2.4. Spectra data

The isolated compounds were structurally elucidated by means of 1D, 2D NMR and mass spectrometry as well as by comparison of the corresponding spectral data with those of literature. The NMR assignment of these compounds is shown in supplementary Table S1–13.

2.5. In vitro enzyme inhibitory assays

2.5.1. In vitro α-amylase inhibitory

The α-Amylase inhibitory potential of compound 1–13 was evaluated as described by [25] with slight modification. Briefly, in a 96-well plate, 50 μL of phosphate buffer (50 μL, 100 mM, pH = 6.8), 10 μL of α–amylase (2 U/mL), and 20 μL of varying concentrations of pure isolated compounds (0.1, 0.2, 0.3, 0.4, and 0.5 mg/mL) were pre incubated at 37 °C for 20 min. Then, 20 μL of 1% soluble starch (100 mM phosphate buffer pH 6.8) was added as a substrate and incubated further at 37 °C for 30 min; 100 μL of the DNS color reagent was then added and boiled for 10 min. The absorbance of the resulting mixture was measured at 540 nm using Multiplate Reader (Multiskan thermo scientific, version 1.00.40). Acarbose at various concentrations (0.1–0.5 mg/mL) was used as a standard. The isolated compounds were set up in parallel as control and each experiment was performed in triplicates. The results were expressed as percentage inhibition, which was calculated using equation:

$$\alpha - \text{amylase inhibitory activity } (\%) = \left(1 - \frac{As}{Ac}\right) \times 100$$

Where,

A_s is the absorbance in the presence of test compound and Ac is the absorbance of control.

2.5.2. In vitro α-glucosidase inhibitory activity

α-Glucosidase inhibitory activity of isolated compounds was carried out according to the standard method [26] with minor modification. In a 96-well plate, reaction mixture containing 50 μL phosphate buffer (100 mM, pH = 6. 8), 10 μL α-glucosidase (1 U/mL), and 20 μL of varying concentrations of pure compounds (0.1, 0.2, 0.3, 0.4, and 0.5 mg/mL) was pre incubated at 37 °C for 15 min. Then, 20 μL P-NPG (5 mM) was added as a substrate and incubated further at 37 °C for 20 min. The reaction was stopped by adding 50 μL Na_2CO_3 (0.1 M). The absorbance of the released p-nitrophenol was measured at 405 nm using Multiplate Reader. Acarbose at various concentrations (0.1–0.5 mg/mL) was included as a standard. Without test substance was set up in parallel as a control and each experiment was performed in triplicates. The results were expressed as percentage inhibition, which was calculated using the following equation:

$$\alpha - \text{glucosidase inhibitory activity } (\%) = \left(1 - \frac{As}{Ac}\right) \times 100$$

Where, A_s is the absorbance in the presence of test compound and A_c is the absorbance of control.

2.6. Molecular docking

The chemical structures of the characterized 13 phytocompounds isolated from the leaves and root barks of *S.latifolius* were drawn using the ChemDraw 22.0.0 software and they were imported in SMILES formats into the workspace of the Maestro 12.2 for preparation using the LigPrep programme (LigPrep, Schrodinger, LCC, New York, NY, 2019). The adopted preparation protocols include the protonation state assignment by Epik at a pH of 7.0 ± 2.0, estimation of geometry and partial atomic charges using OPLS-3e force field, energy minimization and other settings at default. The prepared energy-minimized ligand conformers were saved in the LigPrep output folder accordingly for docking [27].

The crystal structures of the α-amylase with a nitrite-acarbose complex and maltase-glucosidase (MGAM) in complex with an inhibitor, acarbose were retrieved from the Research Collaboratory for Structural Bioinformatics Protein Data Bank (RCSB PDB, https://www.rcsb.org/) to represent the human pancreatic α-amylase and α-glucosidase respectively for docking analysis. They are annotated as PDB ID: 2QV4 (Maurus et al., 2008) and PDB ID: 3TOP (Ren et al., 2011). They were equally prepared for docking using the Protein Preparation programme and active Receptor Grid pocket generation available in the Maestro 12.12 software. The procedures were followed according to some relevant reports [27–29].

The prepared ligand conformers were docked against the prepared enzyme structures to theoretically evaluate their inhibitory binding and interactive potentials at the active pockets of the enzymes, in comparison with a renowned co-crystallized inhibitor, acarbose. The docking analysis was carried out in Maestro 12.12 software (Ligand docking, Schrodinger, LCC, New York, NY, 2019), adopting relevant procedures [27,28]. The ligand-enzyme docking complexes were ranked according to the binding energy scoring functions and 2D interaction diagrams with essential amino acid residues at the active sites of the enzymes. The docking analysis, being a theoretical study was validated by removing the co-crystallized ligand, acarbose from the active binding pocket of the human α-amylase (PDB ID 2QV4) and redocking the ligand onto the same pocket. Both originally co-crystallized and redocked acarbose were then superimposed followed by the estimation of their RMSD. A RMSD value of <2.0 Å validates the protocol as precise and reliable [30,31].

2.6.1. Prediction of physicochemical, pharmacodynamics and pharmacokinetics of isolated compounds

The druggability and toxicological profiles of the isolated compounds in terms of absorption, distribution, metabolism, excretion and toxicity (ADMET) were predicted using the freely accessible Swissadme server (http://www.swissadme.ch/) [32]. The predicted parameters include molecular weight (MW), number of H-bond acceptor (HBA), H-bond donors (HBD) and rotatable bonds, topological polar surface area (TPSA), partition coefficient (Consensus Log P), solubility class (ESOL), gastrointestinal (GI) absorption, substrate/inhibitor of permeability glycoprotein (P-gp), permeability through the blood-brain barrier (BBB), skin permeability (Log Kp) and susceptibility to metabolic cytochrome P450 enzymes inhibition, all benchmarked with the Lipinski's rule of five (RO5) accordingly [33].

3. Results and discussion

3.1. Structure elucidation of the isolated compounds

Purification of crude extracts of leaves and rootbarks of *S.latifolius* had resulted into isolation of pure phytochemicals. Four phytochemicals (1–4) were isolated from the leaves extract while nine phytochemicals (5–13) from the root-barks extract. The compounds were structurally elucidated by means of 1D, 2D NMR and mass spectrometry as well as by comparison of the corresponding spectral data with those of literature. The structures of these compounds are shown in Fig. 1.

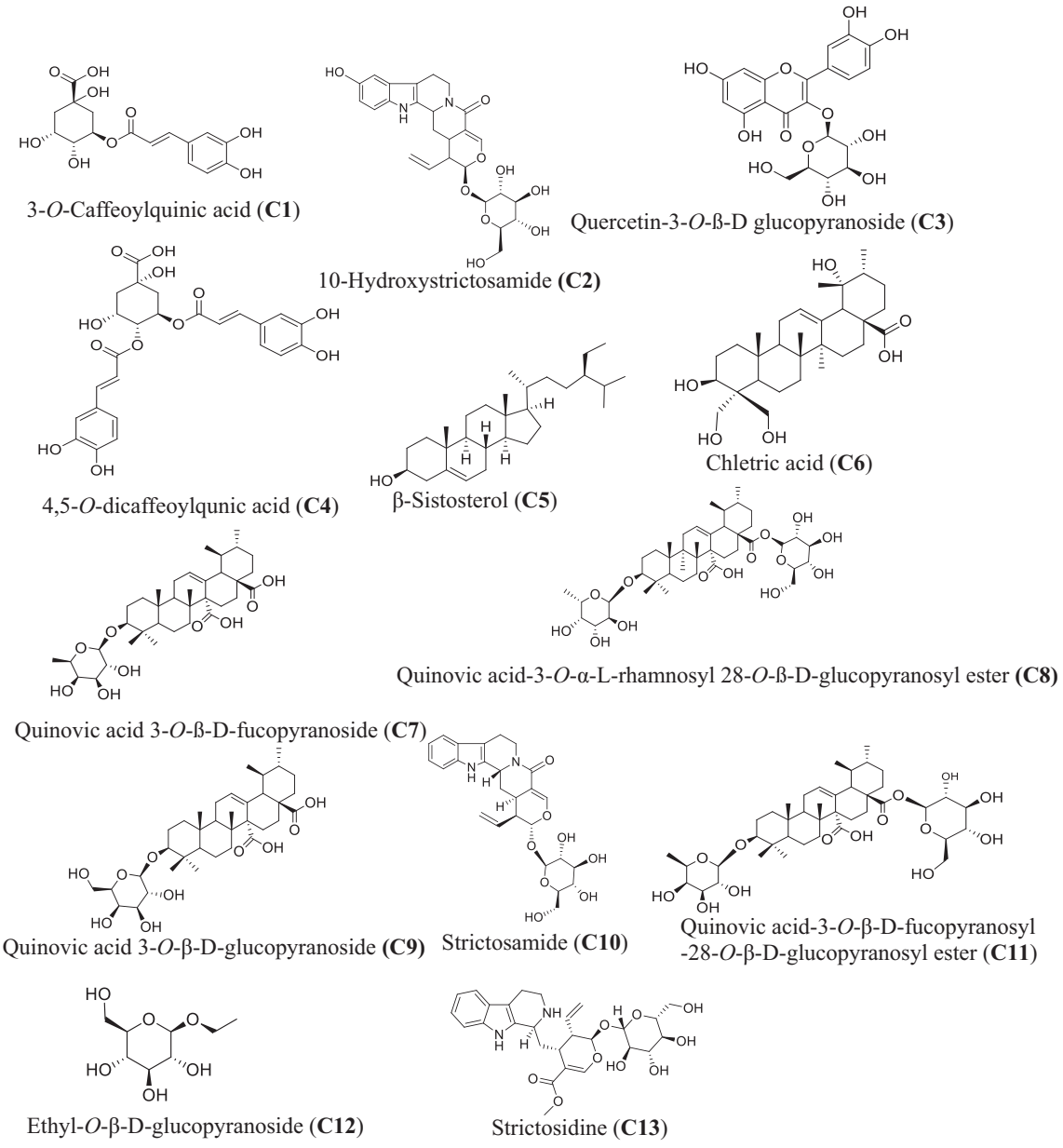


Fig. 1. Chemical structures of 13 compounds isolated from *S. latifolius*.

In this study, various phytochemicals, including phenolic acids, flavonoid glycosides, monoterpene indole alkaloids, saponins (both mono and bis-desmosides), pentacyclic triterpenoids, and steroids were isolated and structurally identified from the leaves and rootbark of *S. latifolius*. Subsequently, the *in vitro* enzymes inhibitory effects on these isolated compounds were assessed against α-amylase and α-glucosidase. More so, to gain insights into the mechanistic aspects of these interactions, docking analysis was employed to observe how the selected compounds bind to the active site residues of both enzymes. Additionally, the druggability and toxicity of the selected compounds were predicted, aligning with previous relevant studies [34]. The structural identification of these compounds is detailed below.

Compound **1** was isolated as a light brown amorphous powder (0.0020%) and identified as 3-*O*-Caffeoylquinic acid. Its molecular formula $C_{16}H_{18}O_9$ was determined by the positive ESI-MS *m/z* 393.300 [M + K] $^+$ 377.087 [M + Na]$^+$, 355.170 [M + H]$^+$ (calcd. For [M+ H] $^+$, 355.170). The ^{1}H and ^{13}C NMR spectra data (S1) of compound **1** (Table S1) corresponds to the report of [35] who isolated the compound from *Euonymus alatus*. Compound **2**, (10-hydroxystrictosamide) was isolated as a yellow amorphous powder (0.0026%) and found to have a molecular mass of 514.1951 [M + H] $^+$, corresponding to the molecular formula $C_{26}H_{30}N_2O_9$ (Fig. 1). The ^{1}H (S2) and ^{13}C NMR spectra data for compound 2 (Table S2) agreed with the reported data [36]. Compound **3** was obtained as a yellow amorphous powder (0.0098%) and characterized by molecular mass 463.008 [M + H] $^+$, corresponding to a molecular formulae $C_{21}H_{20}O_{12}$, and was identified as quercetin-3-*O*-β-D-glucopyranoside (Fig. 1). The ^{1}H (S3) and ^{13}C NMR spectra data (Table S3) matched the report of Pratima and Sonal [37], who isolated the compound from *Azadirachta indica*. Compound **4,** 4,5-*O*-Dicaffeoylquinic acid (Fig. 1), characterized by molecular mass *m/z* 516 [M + H] $^+$ was isolated as a light brown amorphous powder (0.00033%). ^{1}H NMR (S4) and DEPTQ-135^0 spectra (Table S4) are in good agreement with the reported data of Nadia et al., [38] who isolated the compound from *Artemisia capillaris*. Compound **5** was isolated as a white crystalline substance (0.005%). Its ^{1}H NMR spectrum (S5) agreed with report of [39] (Table S5) and the compound was identified as β-sitosterol (Fig. 3). Compound **6** was isolated as a light-yellow solid powder (0.0036%). The ^{1}H (S6) and ^{13}C NMR spectra (Table S6) agree with the reported data of

Takahashi and Takani [40] and was identified as chletric acid. Compound **7** was isolated as a light-yellow amorphous powder (0.0013%) and its molecular formula $C_{36}H_{56}O_9$ was deduced from the EI-MS *m/z* 667.367[M + Cl] $^+$ spectrum. Its ^{1}H NMR (S7) and ^{13}C NMR spectra (Table S7) closely matches with the reported data of [41] Thus, the structure of compound **7** was identified as Quinovic acid-3-*O*-β-D-fucopyranoside. Compound 8 was isolated as a pale-yellow amorphous powder (0.0011%). The ESI-MS spectrum gave a pseudo molecular anion peak at *m/z* 829.424[M + Cl]$^-$ corresponding to the molecular formula $C_{42}H_{66}O_{14}$ which was confirmed by NMR data. Its ^{1}H NMR (S8) and ^{13}C NMR spectra (Table S8) agreed with the reported data of [42] who isolated the compound from the bark of *Bhesa paniculate*. Compound **9** (quinovic acid-3-*O*-β-D-glucospyranoside) was isolated as a pale-yellow amorphous powder (0.0012%). Its ESI-MS spectrum gave a pseudo molecular anion peak at *m/z* 683.359[M + Cl]$^-$ corresponding to the molecular formula $C_{36}H_{56}O_{10}$ which was confirmed by NMR data. The ^{1}H NMR (S9) and ^{13}C NMR spectra of **9** (Table S9) are in good agreement with the reported data of [43] who isolated the compound from *Nauclea diderrichii*. Compound **10** was isolated as a yellow amorphous powder (0.013%). Its ESI-MS spectrum revealed a pseudomolcular ion peak [M + H] $^+$ at *m/z* 499.208 corresponding to the molecular formula of $C_{26}H_{30}N_2O_8$ and identified as strictosamide. The ^{1}H (S10) and ^{13}C NMR spectra (Table S10) of Compound **10** are in good agreement with the reported data of [44] who identified the compound from the bark of *Nauclea orientalis*. Compound 11 was isolated as a yellow amorphous powder (0.0014%) and its ESI-MS showed a pseudo molecular ion at *m/z* 829.420[M + Cl]$^-$. Its molecular formula was established as $C_{42}H_{66}O_{14}$ and was elucidated as quinovic acid 3-*O*-β-D-fucopyranosyl-28-β-D-glucopyranosyl ester. The ^{1}H NMR (S11) and ^{13}C NMR spectra (Table S11) of compound 11 matched with the reported data of [45] who identified the compound from *Uncarla tomentosa* and *Guettarda platypoda*. Although information on its ^{1}H NMR data is scarce from literature. Compound 12 was obtained as a colourless gummy substance (0.0027%). The ESI-MS spectrum gave a pseudo molecular anion peak at *m/z* 243.066 [M + Cl]$^-$ corresponding to the molecular formula $C_8H_{16}O_6$ which was confirmed by ^{1}H NMR (S3) and ^{13}C NMR spectra data (Table S12). The compound was elucidated and identified as Ethyl-*O*-β-D-glucopyranoside. Compound 13 was isolated as a yellow amorphous powder (0.0032%) and was identified as Strictosidine. Its ESI-MS spectrum revealed a pseudomolcular ion peak m/*z* 575.225 [M + COOH] $^+$ (calculated for $C_{27}H_{34}O_9$ + COOH, 575.225). The ^{1}H NMR (S13) and ^{13}C NMR spectra (Table S13) by comparison with a literature, the spectra data were in full agreement with the reported data of [46] who isolated and identified the compound from *Palicourea crocea* and *Palicourea padifolia*. The chemical structures of the isolated compounds as elucidated are presented in Fig. 1.

3.2. In vitro enzyme inhibitory activities of the isolated compounds

The isolated compounds (1−13) exhibited a range of inhibitory effects on α-amylase and α-glucosidase in a concentration-dependent manner comparable to the standard drug, acarbose. The IC_{50} values for each compound are shown in Table 1.

The inhibitory potential of compounds isolated from leaf extract (1–4) and root bark extract (5–13) of *S. latifolius*, as depicted in Table 1, was assessed against α-amylase and yeast α-glucosidase. These evaluations were made in comparison with the standard antidiabetic drug, acarbose. Compounds 1–4 exhibited potent inhibition of α-amylase, with IC_{50} values of 3.67 ± 0.001, 0.52 ± 0.003, 3.61 ± 0.002, and 3.73 ± 0.003 μg/mL, respectively. Compound 2 demonstrated high potent inhibition of α-amylase compared to other compounds and the standard drug, acarbose (3.65 ± 0.001 μg/mL). Furthermore, these compounds demonstrated substantial inhibitory activity against α-glucosidase, with IC_{50} values of 5.30 ± 0.002, 2.27 ± 0.001, 6.98 ± 0.001, 4.63 ± 0.005 μg/mL, respectively, comparable to the standard drug, acarbose (0.86 ± 0.002 μg/mL). Compounds 5–13 displayed inhibitory activity against both α-amylase and α-glucosidase, with IC_{50} values ranging from 4.18 to 12.88 μg/mL and 0.098 to 3.78 μg/mL, respectively.

Table 1
in vitro Enzymes inhibitory activities of the Isolated Compounds.

	SAMPLE	α-amylase (IC_{50} μg/mL)	α-glucosidase (IC_{50} μg/mL)
1.	5-*O*-Dicaffeoylquinic acid (1)	3.67 ± 0.001	5.30 ± 0.002
2.	10-Hydroxystrictosamide (2)	0.52 ± 0.003	2.27 ± 0.001
3.	Quercetin-3-*O*-glucopyranoside (3)	3.61 ± 0.002	6.98 ± 0.001
4.	4,5-O-Dicaffeoylquinic acid (4)	3.73 ± 0.003	4.63 ± 0.005
5.	β-Sistosterol (5)	8.20 ± 0.010	2.53 ± 0.006
6.	Clethric acid (6)	7.99 ± 0.016	2.57 ± 0.003
7.	Quinovic acid-3-O-β-D-fucopyranoside **(7)**	8.57 ± 0.006	2.42 ± 0.001
8.	Quinovic acid-3-O-α-L-rhamnopyranosyl 28-*O*-β-D-glucopyranoside (8)	4.18 ± 0.004	0.098 ± 0.016
9.	Quinovic acid-3-*O*-β-D-glucopyranoside (9)	5.47 ± 0.003	2.21 ± 0.006
10.	Strictosidine (10)	6.67 ± 0.002	2.74 ± 0.010
11.	Quinovic acid-3-*O*-β-D-fucopyranosyl 28-O-β-D-glucopyranoside (11)	12.88 ± 0.012	2.60 ± 0.002
12.	Ethyl-*O*-β-D-glucopyranoside (12)	7.54 ± 0.012	3.78 ± 0.012
13	Strictosidine (13)	5.92 ± 0.003	2.56 ± 0.003
	Acarbose	3.65 ± 0.001	0.86 ± 0.002

3.3. Molecular docking study of the isolated compounds

The docking protocol was validated by a RMSD value of 1.61 Å estimated from the superimposition of both co-crystallized and redocked acarbose at the active binding pocket of the human α-amylase crystal structure (PDB ID 2QV4) (Supplementary Fig. S14). Table 2 presents the docking binding energies of the isolated compounds with α-amylase (PDB ID: 2QV4) and α-glucosidase (PDB ID: 3TOP), using acarbose as the reference drug. The 2D interaction diagrams of isolated compounds 2 and 13 with the active site residues of α-amylase (PDB ID: 2QV4) and α-glucosidase (PDB ID: 3TOP) are depicted in Fig. 2.

The molecular docking procedure was validated as precise and reliable by an RMSD value of 1.61 Å accordingly, [30,31] when the co-crystallized ligand, acarbose and its redocked form were superimposed at the active binding site of the crystal structure of human α-amylase (PDB ID: 2QV4). From other docking results by scoring algorithm (Table 2), acarbose showed highest and second to the highest scores with their theoretical binding affinities of −8.515 and − 7.631 kcal/mol against the human pancreatic α-amylase and α-glucosidase respectively. Among the phytochemicals under probe, compound 2 has the next

Table 2
The docking binding energies of the isolated compounds with α-amylase (PDB ID: 2QV4) and α-glucosidase (PDB ID: 3TOP).

Human pancreatic α-amylase (PDB ID: 2QV4)		Human maltase-glucoamylase PDB ID: 3TOP	
Title	Docking score (kcal/mol)	Title	Docking score (kcal/mol)
		Compound 13	**−7.791**
Acarbose_R2	**−8.515**	**Acarbose_R2**	**−7.631**
Compound 2	**−7.970**	Compound 4	−6.144
Compound 10	−6.409	Compound 2	−5.852
Compound 13	−6.331	Compound 12	−5.665
Compound 6	−5.666	Compound 1	−5.458
Compound 1	−5.638	Compound 8	−5.456
Compound 4	−5.622	Compound 3	−4.897
Compound 12	−5.451	Compound 7	−4.769
Compound 3	−5.415	Compound 9	−4.715
Compound 8	−5.218	Compound 11	−4.715
Compound 9	−4.941	Compound 10	−4.705
Compound 11	−4.941	Compound 6	−4.157
Compound 5	−4.374	Compound 5	−3.311
Compound 7	−4.256		

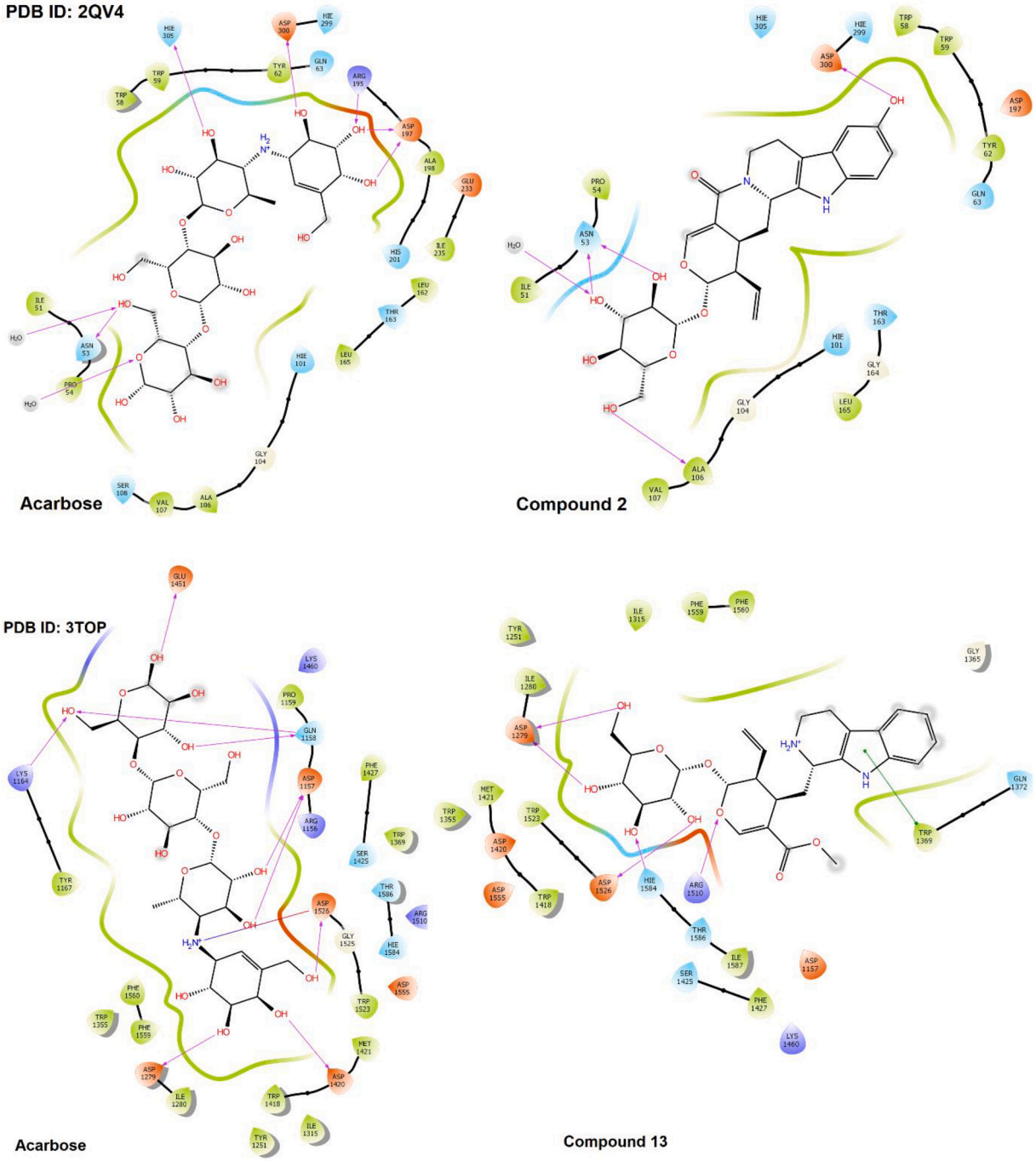


Fig. 2. 2D interaction diagrams of isolated compounds 2 and 13 with the active site residues of α-amylase (PDB ID: 2QV4) and α-glucosidase (PDB ID: 3TOP). Interactions: H-bonding (magenta arrow), salt bridge (red-blue line), π - cation (blue line) and π - π stacking (green line). (For interpretation of the references to color in this figure legend, the reader is referred to the web version of this article.)

highest score to acarbose with −7.970 kcal/mol against the α-amylase and a good score of −5.852 kcal/mol against the α-glucosidase. The compound displayed a strong binding affinity against the human α-amylase, comparably to the standard drug, acarbose. Similarly, compound 13 showed a higher score of −7.791 kcal/mol than acarbose standard and compound 2 against the α-glucosidase and equally a good binding score of −6.331 kcal/mol against the α-amylase. These indicate the potential for strong inhibitory binding to the enzymes as experimentally validated in the results in Table 1. For instance, compound 2 showed the highest antihyperglycemic potential *in vitro* along the α-amylase pathway with the lowest IC_{50} value of 0.52 ± 0.003 μg/mL against the enzyme and an impressive IC_{50} value of 2.27 ± 0.001 μg/mL against the α-glucosidase.

3.4. *In silico* ADMET predictions

The *in silico* ADMET predictions of the selected compounds 2 and 13 are shown in the Table 3 and Supplementary Table S1. These displayed the predicted parameters that characterize the ADMET and druggability of the isolated compounds. Majority of these compounds, particularly the selected compounds 2 and 13, obey the Lipinski's Rule of Five with few or no violations. The bioavailability radars of the selected compounds 2 and 13 in comparison with acarbose is shown in Fig. 3, based on their predicted physicochemical profiles.

Table 3
In silico ADMET predictions of the selected compounds 2 and 13.

Molecule	Compound 2	Compound 13	Acarbose
MW	514.52	530.57	645.6
#Rotatable bonds	4	8	9
#H-bond acceptors	9	10	19
#H-bond donors	6	6	14
TPSA	164.94	162.73	321.17
Consensus Log P	0.11	0.64	−6.22
ESOL Class	Soluble	Soluble	Highly soluble
GI absorption	Low	Low	Low
BBB permeant	No	No	No
Pgp substrate	Yes	Yes	Yes
CYP1A2 inhibitor	No	No	No
CYP2C19 inhibitor	No	No	No
CYP2C9 inhibitor	No	No	No
CYP2D6 inhibitor	No	No	No
CYP3A4 inhibitor	No	No	No
log Kp (cm/s)	−9.4	−9.11	−16.29
Lipinski #violations	3	3	3
Synthetic Accessibility	5.81	6.04	7.34

The interaction diagrams of the human pancreatic α-amylase (PDB ID: 2QV4) in complexes with the top-ranked compound 13 in terms of the docking score and that of the co-crystallized ligands are presented in Fig. 2. Accordingly, three residues are critical for the catalytic activities of the enzyme. These are Asp 197 as a catalytic nucleophile renowned for displacing the aglycon of glucosidic substrates, Glu 233 representing an acid/base catalytic residue for aiding stabilization states during substrate hydrolysis and Asp 300 important for conformational stabilization of bound substrates [4]. Three other residues, Arg 195, Asn 298 and Arg 337 are directly functional binders of Cl ion and water molecules for catalytic processes. In addition, Arg 195 forms side-chain interactions with Asp 197 and Glu 233, thereby aiding their catalytic activities. Together with His 299 and Asp 300, the amino acid residue supports the binding of glucose substrate at the subsite −1 for the catalytic attack by Asp 197 during enzymatic hydrolysis [4]. As such, binding of bioactive agents to these residues remains pivotal for an effective inhibition of the enzyme. The renowned inhibitor, acarbose, co-crystallized with the enzyme showed very strong interactions with these critical residues and others. These include H-bonding interactions with Asn 53, Arg 195, Asp 197, Asp 300, His 305 and some water molecules, as well as hydrophilic van der Waal's interactions with Glu 233 and 299. Similarly, the top-ranked compound 2 against the enzyme interacted with Asn 53, Ala 106, Asp 300 and some water molecules while residues such as Asp 197, His 299 and His 305 formed hydrophilic van der Waal's interactions with the compound. According to the authors of the crystal structure (PDB ID: 3TOP), the residues that constitute the active catalytic site of the enzyme include Asp 1157, Tyr 1251, Asp 1279, Trp 1355, Trp 1418, Arg 1510, Trp 1523, Asp 1526, Phe 1559 and Phe 1560 [4]. From the 2D binding interaction diagrams (Fig. 2), the co-crystallized inhibitor, acarbose showed an H-bonding to a critical acid/base catalytic residue, Asp 1526 *via* the N4B of the acarbose moiety. It also displayed strong H-bonding interactions with Asp 1157 and Asp 1279, and hydrophobic interactions with Tyr 1251, Trp 1418 and Trp 1523. These are important for the stabilization of its sugar ring, consistently with the crystal structure [5], thereby validating the docking protocol. Similarly, compound 13 strongly interacted with Asp 1279, Asp 1526 and Arg 1510 through H-bondings to one or more of its OH/O moieties. In addition, the compound engaged in hydrophobic π-π stacking with Trp 1369 at the subsite 2 consistently with the co-crystallized acarbose. The similarities between the co-crystallized and redocked acarbose and the isolated compound 13 in terms of bonding and non-bonding interactions with the active residues at the catalytic pocket of α-glucosidase potentiate similar inhibitory effects upon experimentation. More importantly, the consistency between the docking results and *in vitro* experimental IC_{50} values, portraying inhibitory effects of the selected phytocompounds on the enzymes in comparison with a standard inhibitor has been similarly reported for some bioactive compounds as promising antidiabetics [47,25,48]. These strongly support the inclusion of the highlighted compounds being probed in such interesting pools of putative antihyperglycemic candidates for further translational studies as future antidiabetics.

The predicted parameters that define the ADMET and druggability of the isolated compounds are presented in Table 3 and Supplementary Table S1. Most of the isolated compounds, especially the selected compounds 2 and 13 obey Lipinski's RO5 with insignificant violations. This is indicated by MW $\leq$ 500 Da; the number of rotatable bonds RB $\leq$ 10; HBA $\leq$ 10, HBD $\leq$ 5 and partition coefficient log $P \leq 5$, thereby supporting their promising physicochemical and pharmacokinetic properties for druggability [34,49]. Additionally, the TPSA supports the intestinal absorption and permeability of BBB [50]. Although, the predicted TPSA values for the isolated compounds range from 20.23 to 232.90 Å with some few falling outside the preferable range (70–140 Å). However, this may not significantly affect their druggability, especially since the reference standard drugs, montbretin A and acarbose, have higher TPSA values of 533.18 Å and 321.17 Å respectively. Thus, the selected compounds display good scores for lipophillicity, flexibility, unsaturation, solubility, size and polarity for ideal bioavailability in better terms than the reference acarbose (Fig. 3). Interestingly, they are mostly predicted with good solubility indices comparably to the reference drugs with few exceptions in compounds 5, 7, 9 and 11. Again, the compounds show a weak potential for GI absorption, BBB permeation and more interestingly no inhibitory potentials to the super metabolic CYP enzymes, consistently with acarbose, indicating their promising safety and low toxicological effects. Finally, they have a high synthetic

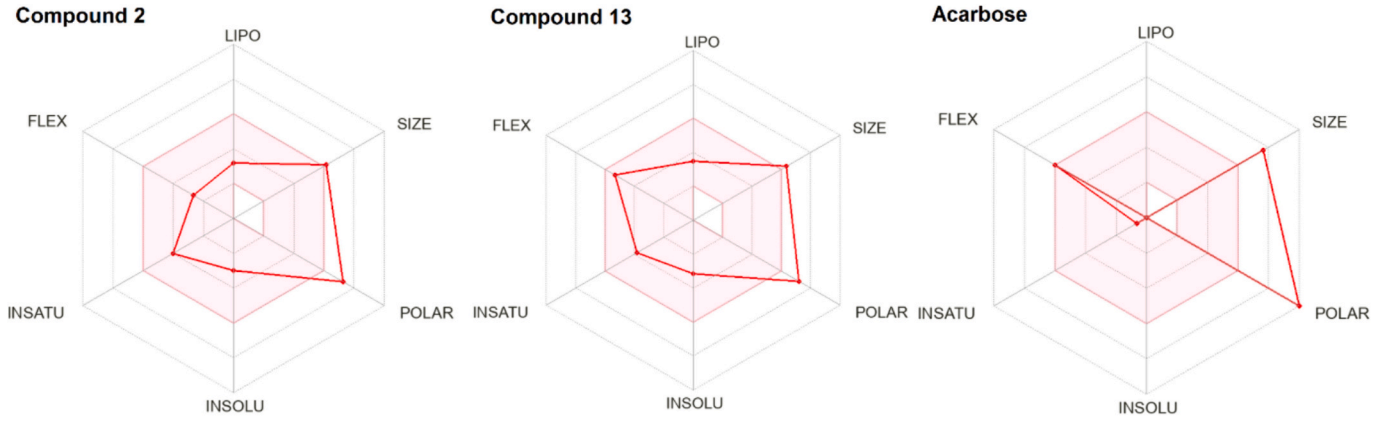


Fig. 3. Bioavailability radar of selected compounds 2 and 13 in comparison with acarbose. The selected isolated compounds express ideal flexibility, lipophillicity, size, solubility and polarity, supporting their bioavailability in better terms than acarbose.

accessibility for ease of derivatization and structure-activity relationship modification.

4. Conclusion

The present study isolated and characterized total number of thirteen (13) bioactive compounds from the leaves and rootbarks extracts of *S. latifolius*. These compounds were evaluated for their potential to inhibit α-amylase and α-glucosidase enzymes. All isolated compounds demonstrated potent inhibition of α-amylase and α-glucosidase comparably to the reference inhibitor, acarbose. However, the synergistic effects of these compounds in plant may enhance their inhibitory actions on these enzymes, making them promising candidates for anti-hyperglycemia agents. The molecular docking analysis revealed that compounds 2 and 13 had high binding affinity with α-amylase, comparably to acarbose, and also exhibited favourable interactions with α-glucosidase. Additionally, all the isolated compounds demonstrated ideal ADMET properties, indicating good bioavailability and low toxicity potential. This research highlights the potential of compounds from *S. latifolius* as promising candidates for the development of novel anti-hyperglycemic agents, particularly compounds 2 and 13, which showed remarkable inhibitory activity against α-amylase and favourable binding affinities. In future studies, the mode of inhibition by the selected compounds as competitive, uncompetitive or non-competitive deserves to be assessed through kinetic evaluation. The study advances the search for potent natural product inhibitors of α-amylase and α-glucosidase for effective management of diabetes upon further evaluation.

Funding

A.T.Ajiboye is grateful to the support of Tertiary Education Fund (TETFUND) for research bench work at The National Centre for Natural Products Research, School of Pharmacy, University of Mississippi, United States.

CRediT authorship contribution statement

Abdulfatai Temitope Ajiboye: Writing – original draft, Methodology, Conceptualization. **Olayinka Taiwo Asekun:** Writing – review & editing, Supervision. **Yusuf Oloruntoyin Ayipo:** Writing – review & editing, Writing – original draft, Software. **Mohd Nizam Mordi:** Software, Conceptualization. **Oluwole Babafemi Familoni:** Supervision, Conceptualization. **Zulfiqar Ali:** Supervision, Resources, Methodology, Conceptualization. **Ikhlas A. Khan:** Supervision, Resources, Conceptualization.

Declaration of competing interest

The authors declare that they have no known competing financial interests or personal relationships that could have appeared to influence the work reported in this paper.

Acknowledgements

We would like to express our sincere thanks to Prof. Ikhlas A. Khan, National Center for Natural Products Research, School of Pharmacy, University of Mississippi, and University, MS, 38677, United States for the research facilities.

Appendix A. Supplementary data

Supplementary data to this article can be found online at https://doi.org/10.1016/j.fitote.2024.106037.

References

[1] R.A. Alhazzaa, T. Heinbockel, A.B. Csoka, Diabetes and Epigenetics, in: Epigenetics to Optogenetics - A New Paradig. Study Biol, Intech Open, 2021, pp. 1–15. https://www.intechopen.com/books/advanced-biometric-technologies/liveness-detection-in-biometrics.

[2] P. Saeedi, I. Petersohn, P. Salpea, B. Malanda, S. Karuranga, N. Unwin, S. Colagiuri, L. Guariguata, A.A. Motala, K. Ogurtsova, J.E. Shaw, D. Bright, R. Williams, Global and regional diabetes prevalence estimates for 2019 and projections for 2030 and 2045: results from the international diabetes federation diabetes atlas, 9th edition, Diabetes Res. Clin. Pract. 157 (2019) 107843, https://doi.org/10.1016/j.diabres.2019.107843.

[3] R.A. MaurusBegum, L.K. Williams, J.R. Fredriksen, R. Zhang, S.G. Withers, G. D. Brayer, Alternative catalytic anions differentially modulate human R -amylase activity and specificity, Biochemistry 47 (2008) 3332–3344.

[4] L. Ren, X. Qin, X. Cao, L. Wang, F. Bai, G. Bai, Y. Shen, Structural insight into substrate speci ficity of human intestinal maltase-glucoamylase, Protein Cell 2 (10) (2011) 827–836, https://doi.org/10.1007/s13238-011-1105-3.

[5] R. Hu, Y. Li, Q. Lv, T. Wu, N. Tong, Acarbose monotherapy and type 2 diabetes prevention in eastern and Western prediabetes: an ethnicity-specific Meta-analysis, Clin. Ther. 37 (8) (2015) 1798–1812, https://doi.org/10.1016/j.clinthera.2015.05.504.

[6] J. Vasanthkumar, A. Hulikal, S. Santoshkumar, H. Sripathy, In silico docking studies of α - amylase inhibitors from the anti - diabetic plant Leucas ciliata Benth and an endophyte, *Streptomyces longisporoflavus*, 3 Biotech 11 (2) (2021) 1–16, https://doi.org/10.1007/s13205-020-02547-0.

[7] A. Isman, A. Nyquist, M. Moel, X. Zhang, S. Zalzala, The efficacy and tolerability of intermittent prandial acarbose to reduce glucose spikes in healthy individuals, Transl. Med. Aging 7 (2023) 12–19.

[8] Z.R. Li, R.B. Jia, J. Wu, L. Lin, Z.R. Ou, B. Liao, L. Zhang, X. Zhang, G. Song, M. Zhao, Sargassum fusiforme polysaccharide partly replaces acarbose against type 2 diabetes in rats, Int. J. Biol. Macromol. 170 (2021) 447–458, https://doi.org/10.1016/j.ijbiomac.2020.12.126.

[9] Y. Dong, L. Sui, F. Yang, X. Ren, Y. Xing, Z. Xiu, Reducing the intestinal side effects of acarbose by baicalein through the regulation of gut microbiota: an in vitro study, Food Chem. (2021) 394133561, https://doi.org/10.1016/j.foodchem.2022.133561.

[10] A. Gidado, D.A. Ameh, S.E. Atawodi, Effect of *Nauclea latifolia* leaves aqueous extracts on blood glucose levels of normal and alloxan-induced diabetic rats, Afr. J. Biotechnol. 4 (2005) 91–93.

[11] O.E. Ette, P.M.E. Ubulom, C.E. Ekpenyong, U.S. Ekong, O.E. Akpan, V.D., Tambari *in vivo* antiplasmodial activities of Nauclea latifolia, Asian J. Med. Sci. 3 (6) (2015) 6–11.

[12] A.T. Ajiboye, O.T. Asekun, O.B. Familoni, HPLC profile of phenolic contents, antioxidant and antidiabetic activities of Methanolic extract of the leaves of *Sarcocephalus latifolius* (Bruce, smith) grown in north central geopolitical zone, Nigeria, J. J. Chem. 15 (03) (2020) 95–101.

[13] S.A. Aderibigbe, S.O. Idowu, A.A. Olaniyi, C.W. Wright, A.A. Fatokun, Bioactivity and cytotoxicity profiling of strictosamide and vincosamide, anthelmintic epimers from *Sarcocephalus latifolius* (smith) Bruce leaf, J. Ethnopharmacol. 265 (2020) 113142.

[14] A.T. Ajiboye, M.D. Musa, K.O. Otun, A.A. Jimoh, A.T. Bale, M.T. Arowona, The studies of antioxidant and antimicrobial potentials of the leaf extract of *Bauhinia monandra* plant, Nat. Prod. Chem. Res. 3 (2015) 180.

[15] A.T. Ajiboye, S.O. Lawal, K.O. Otun, A.T. Bale, M.T. Arowona, Evaluation of physico-chemical and antimicrobia studies of *delonix regia* and *piliostigma thonningii* seed oils. Jourdan, J. Chemother. 12 (1) (2017).

[16] R. Haudecoeur, M. Peuchmaur, B. Pérès, M. Rome, G.S. Taïwe, A. Boumendjel, B. Boucherle, Traditional uses, phytochemistry and pharmacological properties of African Nauclea species: A review, J. Ethnopharmacol. 212 (2018) 106–136.

[17] A.T. Ajiboye, O.T. Asekun, O.B. Familoni, A. Zulfiqar, W.G. Yan-Hong, G. Mustafa, Z. Fazila, L. Christopher, A.S. Odewo, A.K. Ikhlas, Phytochemicals isolated from the root bark of *Sarcocephalus latifolius* (Sm.) E.A.Bruce, Biochem. Syst. Ecol. 86 (2019) 103909.

[18] P. Abreu, A. Pereira, New indole alkaloids from *Sarcocephalus latifolia*, Nat. Prod. Lett. 15 (2001) 43–48.

[19] A. Ata, C.C. Udenigwe, W. Matochko, P. Holloway, M.O. Eze, P.N. Uzoegwu, Chemical constituents of *Nauclea latifolia* and their anti-GST and anti-fungal activities, Nat. Prod. Commun. 4 (9) (2009) 1185–1188.

[20] O.A. Ademola, O.O. Oluwafemi, L.B. Nicole, In vitro study on the antioxidant potentials of the leaves and fruits of Nauclea latifolia, Sci. W. J. 23 (4) (2014) 23–33.

[21] T.I. Edewor, S.O. Owa, S.S. Oladipupo, R.A. Oyelakin, Determination of the Total phenolic, flavonoid contents; antioxidant activity and GC-MS study of the leaves of the medicinal plant *Sarcocephalus latifolius*, Int. J. Pharm. Sci. Rev. Res. 34 (2) (2015) 82–86.

[22] O. Alsiddig, A. Sufyan, A. Amna, Antioxidant activity, acetylcholinesterase inhibitory potential and phytochemical analysis of *Sarcocephalus latifolius* Sm. Bark used in traditional medicine in Sudan, BMC Complement. Altern. Med. 17 (2017) 270.

[23] J.J.K. Bankeu, D.U.K. Kagho, Y.S.F. Fongang, R.M.K. Toghueo, B.M. Mba'ning, G.R. T. Feuya, F.B. Fekam, J.C. Tchouankeu, S.A. Ngouela, N. Sewald, B.N. Lenta, M. S. Ali, Constituents from Nauclea latifolia with anti-*Haemophilus influenzae* type b inhibitory activities, J. Nat. Prod. 82 (2019) 2580–258520.

[24] F. Saleem, K. Mohammed, S. Chigurupati, Y. Andriani, M. Solangi, S. Hameed, A. Abdel, M. Abdel, F. Begum, M. Arif, M. Taha, F. Rahim, T. Sifzizul,

Dicyanoanilines as potential and dual inhibitors of a -amylase and a -glucosidase enzymes : synthesis, characterization, in vitro, in silico, and kinetics studies, Arab. J. Chem. 15 (3) (2022) 103651, https://doi.org/10.1016/j.arabjc.2021.103651.
[25] A.O. Ademiluyi, G. Oboh, Soybean phenolic-rich extracts inhibit key-enzymes linked to type 2 diabetes (α-amylase and α-glucosidase) and hypertension (angiotensin I converting enzyme) *in-vitro*, Exp. Toxicol. Pathol. 65 (2013) 305–309.
[26] L.J. Shai, S.R. Magano, S.L. Lebelo, A.M. Mogale, Inhibitory effects of five medicinal plants on rat alpha- glucosidase: comparison with their effects on yeast alpha-glucosidase, J. Med. Plant Res. 5 (28) (2011) 63–67.
[27] Y.O. Ayipo, I. Ahmad, C.F. Chong, N.A. Zainurin, S.Y. Najib, H. Patel, M.N. Mordi, Carbazole derivatives as promising competitive and allosteric inhibitors of human serotonin transporter: computational pharmacology, J. Biomol. Struct. Dyn. (2023) 1–22, https://doi.org/10.1080/07391102.2023.2198016.
[28] Y.O. Ayipo, I. Ahmad, W. Alananzeh, A. Lawal, Computational modelling of potential Zn-sensitive non- β -lactam inhibitors of imipenemase-1 (IMP-1), J. Biomol. Struct. Dyn. (2022) 1–21, https://doi.org/10.1080/07391102.2022.2153168.
[29] S.G. Madhavi, M. Adzhigirey, T. Day, R. Annabhimoju, W. Sherman, Protein and ligand preparation: parameters, protocols, and influence on virtual screening enrichments, J. Comput. Aided Mol. Des. 27 (3) (2013) 221–234, https://doi.org/10.1007/s10822-013-9644-8.
[30] A. Castro-Alvarez, A.M. Costa, J. Vilarrasa, The performance of several docking programs at reproducing protein-macrolide-like crystal structures, Molecules 22 (1) (2017), https://doi.org/10.3390/molecules22010136.
[31] D. Ramírez, J. Caballero, Is it reliable to take the molecular docking top scoring position as the best solution without considering available structural data, Molecules 23 (5) (2018) 1–17, https://doi.org/10.3390/molecules23051038.
[32] A. Daina, O. Michielin, V. Zoete, SwissADME: a free web tool to evaluate pharmacokinetics, drug-likeness and medicinal chemistry friendliness of small molecules, Sci. Rep. 7 (2017) 1–13, https://doi.org/10.1038/srep42717.
[33] A. NaAllah, Y.O. Ayipo, D.I. Komolafe, S. Solihu, B. Bamidele, M.A. Alabi, A. A. Balogun, A.T. Abdulazeez, M.N. Mordi, Phytochemical screening and in silico pharmacological profiling of ethanolic extract of *Aframomum melegueta* for prostate carcinoma, J. Appl. Pharm. Sci. 11 (7) (2021), https://doi.org/10.7324/JAPS.2021.110715.
[34] F. Saleem, K. Mohammed, S. Chigurupati, Y. Andriani, M. Solangi, S. Hameed, A. Abdel, M. Abdel, F. Begum, M. Arif, M. Taha, F. Rahim, T. Sifzizul, Dicyanoanilines as potential and dual inhibitors of a -amylase and a -glucosidase enzymes : synthesis, characterization, in vitro, in silico, and kinetics studies, Arab. J. Chem. 15 (3) (2022) 103651, https://doi.org/10.1016/j.arabjc.2021.103651.
[35] J. Un-Ho, L. Ji- Young, K. Sung-Koo, K. June-Ki, P. Won-Hwan, M. Jong-Guk K., Sung-Kwon and K. Cheorl-Ho., A phenolic compound, 5-caffeoylquinic acid (chlorogenic acid), is a new type and strong matrix metalloproteinase-9 inhibitor: isolation and identification from methanol extract of *Euonymus alatus*, Life Sci. 77 (2005) 2760–2769.
[36] C.A.J. Erdelmeier, A.D. Wright, J. Orijala, B. Baumgartner, T. Rali, O. Stricher, New indole alkaloid glycosides from *Nauclea orientalis*, Planta Med. 57 (2) (1991) 149–152.
[37] T. Pratima, D.G.S. Sonal, Isolation of quercetin-3-O-β-D-glucoside from *Azadirachta indica*, Am. J. Phytomed. Clin. Ther. 2 (2014) 870–876.
[38] T. Nadia, L. Ji-Hyung, Y. Soon-Ho, J.B. Galzad, J. Da-Woon, R.W. Darren, Isolation of 4,5-*O*-Dicaffeoylquinic acid as a pigmentation inhibitor occurring in *Artemisia capillaris* Thunberg and its validation *in vivo*, Evid. Based Complement. Alternat. Med. (2016) 1–11.
[39] S.C. Venkata, Isolation of Stigmasterol and β-Sitosterol from the dichloromethane extract of *Rubussuavissimus,* Chaturvedula and Prakash, Int. Curr. Pharm. J. 1 (9) (2012) 239–242.
[40] K. Takahashi, M. Takani, Studies on constituents of medicinal plants. XVII. Constituents of Schizandra nigra MAX. and their Carbon-13 nuclear magnetic resonance spectra.(2), Chem. Pharm. Bull. 24 (9) (1976) 2000–2006.
[41] K. Mesia, R.K. Cimanga, L. Dhooghe, P. Cos, S. Apers, J. Totté, G.L. Tona, L. Pieters, A.J. Vlietinck, L. Maes, Antimalarial activity and toxicity evaluation of a quantified Nauclea pobeguinii extract, J. Ethnopharmacol. 19 131(1) (2010) 10–16.
[42] O. Kazuyoshi, T. Hiromi, T. Tatsuya, O. Yasuaki, K. Kazuyoshi, T. Naomi, S. Hirotaka, K. Isao, Indonesian medicinal plants IX. Chemical structures of gongganosides A,B,and C. Three new quinovic acid glycosides from the bark of *Bhesa paniculata* (Celestraceae), Chem. Pham. Bull. 42 (8) (1994) 1596–1600.
[43] M. Lamidi, E. Ollivier, R. Faure, L. Debrauwer, L. Nze-Ekekang, G. Balansard, Quinovic acid glycosides from *Nauclea diderrichii*, Phytochemistry 138 (1) (1995) 209–212.
[44] Z. Zhang, H.N. ElSohly, M.R. Jacob, D.S. Pasco, L.A. Walker, A.M. Clark, New indole alkaloids from the bark of *Nauclea orientalis*, J. Nat. Prod. 64 (2001) 1001–1005.
[45] R. Aquino, F. De Simonec, C. Pizza, Plant metabolites. Structure and *in vitro* antiviral activity of quinovic acid glycosides from *Uncarla tomentosa* and *Guettarda platypoda*, J. Nat. Prod. 52) 4 (1989) 679–685.
[46] B. Andreas, K.K. Maria, I.K. Simon, G. Michael, L. Eberhard, B. Lothar, S. Johann, Loganin and secologanin derived tryptamine–iridoid alkaloids from *Palicourea crocea* and *Palicourea padifolia* (Rubiaceae), Phytochemistry 116 (2015) 162–169.
[47] M. Nawaz, M. Taha, F. Qureshi, N. Ullah, M. Selvaraj, S. Shahzad, S. Chigurupati, A. Waheed, F.A. Almutairi, Structural elucidation, molecular docking, α-amylase and α-glucosidase inhibition studies of 5-amino - nicotinic acid derivatives, BMC Chem. (2020) 1–11, https://doi.org/10.1186/s13065-020-00695-1.
[48] M. Santoso, L. Lin, N. Pasca, F. Ambar, A. Azminah, R. Malina, A. Fadlan, Z.M.A., Judeh synthesis, α-glucosidase inhibition, α-amylase inhibition, and molecular docking studies of 3,3-di(indolyl)indolin-2-ones, Heliyon 8 (2022) e09045, https://doi.org/10.1016/j.heliyon.2022.e09045.
[49] C.A. Lipinski, Avoiding investment in doomed drugs, Curr. Drug Discov. (2001) 117–119.
[50] S. Shayan, S. Jamaran, R.H. Askandar, A. Rahimi, A. Elahi, C. Farshadfar, N. Ardalan, The SARS-Cov-2 Proliferation was blocked by a novel and potent main protease inhibitor via computer-aided drug design, Iran. J. Pharm. Res. 20 (3) (2021) 399.